T

Theta-Gamma Cross-Frequency Analyses (Hippocampus)

Robson Scheffer-Teixeira and Adriano B. L. Tort
Brain Institute, Federal University of Rio Grande do Norte, Natal, RN, Brazil

Synonyms

Amplitude-amplitude coupling; n:m phase-locking; Phase-amplitude coupling; Phase-frequency coupling; Phase-phase coupling

Definition

Brain oscillations of different frequencies can coexist and influence each other. A cross-frequency interaction occurs when a feature from one oscillation (i.e., instantaneous amplitude, phase, or frequency) depends on a feature from another oscillation at a distinct frequency. These phenomena have been collectively called cross-frequency coupling (CFC). There are multiple types of CFC, such as phase-amplitude coupling, amplitude-amplitude coupling, and n:m phase-locking. Several metrics have been devised to quantify CFC.

Detailed Description

The study of the electrical activity produced by the brain dates back to Richard Caton in 1875, who employed a galvanometer to record from the cortex of rabbits (Geddes 1987). Neuronal spikes and extracellular field potentials have been since recorded from several brain regions of different species, and spectral analyses have shown that they are often rhythmical. Scientists usually classify brain oscillations according to their frequency, waveform shape, local of origin, and associated behavior. Among them, the hippocampal formation of rats and mice produces a prominent rhythm in the 4–12 Hz range when animals explore their surroundings or during REM sleep, the so-called theta oscillations (Buzsáki 2002). In addition, faster oscillations appear associated with theta waves, such as gamma rhythms (30–100 Hz) and high-frequency oscillations (HFOs; 120–160 Hz) (Scheffer-Teixeira and Tort 2017). A new field of higher-level analysis emerged with the discovery that oscillations of distinct frequencies might not only coexist but also interact with each other (Canolty and Knight 2010; Hyafil et al. 2015). Oscillatory interaction can occur through any of the main features of a rhythm: amplitude, phase, or frequency (Fig. 1). These phenomena are collectively known as cross-frequency coupling (CFC). To date, the most studied CFC types are phase-amplitude coupling, amplitude-amplitude coupling, and n:m phase-locking,

D. Jaeger, R. Jung (eds.), *Encyclopedia of Computational Neuroscience*,
https://doi.org/10.1007/978-1-4614-7320-6_100658-1

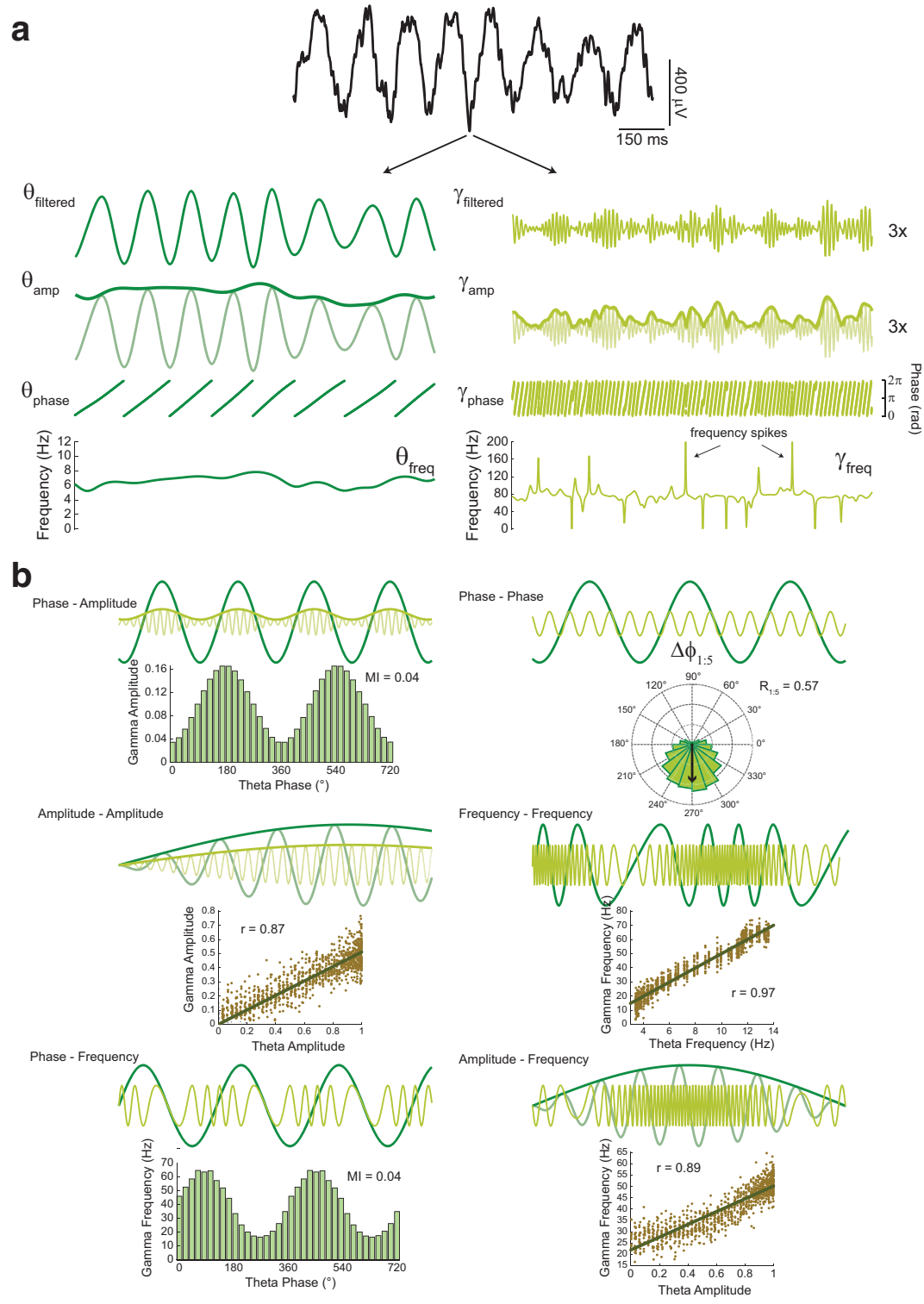

Fig. 1 (continued)

while other CFC types remain to be further explored (Hyafil et al. 2015).

Measures of synchronization between brain waves were first motivated by the study of coupled oscillators (Ermentrout and Kopell 1991; Tass et al. 1998; Strogatz 2000; Rosenblum et al. 2001). However, despite local regularities and short-term predictability, neural oscillations do not behave as stationary sinusoids and are not easily described by a set of equations. Rather, local field potentials (LFPs) are subject to several sources of variability, most unknown or uncontrolled, and exhibit noisy states and chaotic components. While not formally demonstrated, the coupling between brain signals is believed to fall into the category of "weakly coupled oscillators" (Hoppensteadt and Izhikevich 1998). Several approaches were proposed to infer the existence and quantify the degree of coupling based on a general statistical sense: two oscillations are assumed to be coupled if knowledge of the state of one oscillation predicts the state of another oscillation. Notice that this statistical definition ignores the underlying mechanisms. In particular, it does not inform about directionality and causality, that is, whether an oscillation modulates, is modulated, or both, whether coupling is externally or internally driven, direct or indirect.

The following sections summarize common CFC metrics. For simplicity, we often refer to theta and gamma as canonical examples of slow and fast oscillations of interest, but the metrics are general enough to be applied to any cross-frequency pair.

Filtering and Feature Extraction

Phase, frequency and amplitude can be extracted from brain signals (LFP, EEG, MEG) using standard signal processing techniques. The first step is to filter the raw data into the desired frequency range, which can be achieved by many different types of filters. Of note, to detect phase-amplitude coupling, the bandwidth of the filtered fast oscillation component (i.e., gamma) must include its peak frequency (f_γ) and the side-band frequencies at $f_\gamma \pm f_\theta$, where f_θ is the frequency of the slow oscillation (i.e., theta) (Berman et al. 2012; Aru et al. 2015).

After filtering, the phase and amplitude time series can be obtained from its analytic representation, defined as $Z(t) = X(t) + iH(X(t))$, where the real part, $X(t)$, is the filtered signal and the imaginary part, $H(X(t))$, its Hilbert transform, which is a version of $X(t)$ shifted by $-90°$. The instantaneous amplitude at each time t is defined as the absolute value of $Z(t)$, given by $|Z(t)| = \sqrt{X(t)^2 + H(X(t))^2}$, while the instantaneous phase at time t is defined as $\varphi(t) = \tan^{-1}(H(X(t))/X(t))$. Notice that $Z(t)$ can be expressed in polar form as $Z(t) = |Z(t)|e^{i\varphi(t)}$. Alternatively, the amplitude and phase time series can be obtained as the absolute value and angle of a complex wavelet transform (with the due caution of the filtered bandwidth). The instantaneous phase can also be estimated by linear interpolation: peaks and valleys of the filtered signal are first identified and set to predefined phases (e.g., 0° for peak and 180° for valley). Subsequently, the samples between each peak-to-valley and valley-to-peak interval are attributed to linearly spaced phase values (Belluscio et al. 2012).

Finally, the instantaneous frequency is estimated from the first derivative of the unwrapped phase time series: $f(t) = \frac{1}{2\pi}\frac{d\varphi(t)}{dt}$.

CFC Metrics

Several of the metrics below assume that the signal has already been band-pass filtered into the theta and gamma ranges of interest and the relevant features extracted (i.e., phase and amplitude time series). Ideally, the frequency boundaries of

Theta-Gamma Cross-Frequency Analyses (Hippocampus), Fig. 1 Multiple CFC types. (**a**) Feature extraction from a rat LFP epoch containing theta and gamma oscillations during REM sleep. Theta and gamma signals are obtained through band-pass filtering and their phase and amplitude series extracted using the Hilbert transform. The instantaneous frequency time series is derived from the phase time series. (**b**) Each subpanel depicts one possible CFC type by means of simulated data

the band-pass filter should be selected based on visual inspection of the power spectrum, so as to encompass the power "bumps" at the corresponding frequencies. However, while theta is usually associated with a discernable power peak, the frequency boundaries of gamma activity are often difficult to determine due to the much lower signal-to-noise ratio, especially for the faster gamma subbands. In these cases, the choice of the filtered band may be based on the inspection of comodulation maps (see below) or on previous studies.

Phase-Amplitude Coupling (PAC)

PAC has been identified in different types of brain signals and received much attention in recent literature. We summarize some of the PAC metrics in this section (Fig. 2), but we note that the list is nonexhaustive and novel metrics are continuously being devised.

Measures Based on the Maximal and Minimal Values of the Amplitude Distribution

Several PAC metrics require first computing the mean gamma amplitude as a function of the phase of the theta cycle. This is obtained by partitioning theta phases into nonoverlapping bins and calculating the average gamma amplitude (A_j) associated with each phase bin j. Phase bins are usually 10° to 30° wide.

A straightforward metric for PAC strength is obtained by taking the ratio between the maximum (A_{max}) and minimum (A_{min}) average gamma amplitude within the theta cycle (Lakatos et al. 2005):

$$PAC_{strength} = \frac{A_{max}}{A_{min}}$$

Notice that this ratio is not bounded. Other variants include ratios that vary between 0 and 1, such as:

$$PAC_{strength} = \frac{A_{max} - A_{min}}{A_{max}}$$

and

$$PAC_{strength} = \frac{A_{max} - A_{min}}{A_{max} + A_{min}}$$

Modulation Index (MI)

Tort et al. (2008) defined the PAC MI as an adaptation of a phase synchrony metric based on information theory introduced by Tass et al. (1998). The MI first requires normalizing the average amplitude per phase bin (A_j) to generate a discrete probability-like distribution (P):

$$p_j = \frac{A_j}{\sum_{j=1}^{N_b} A_j}$$

whose Shannon's entropy ($H(P)$) is:

$$H(P) = -\sum_{j=1}^{N_b} p_j \log\left(p_j\right)$$

where j indexes the phase bins and N_b is the total number of bins. The PAC MI is obtained as an "inverted" normalization of $H(P)$:

$$PAC_{strength} = MI = \frac{H_{max} - H(P)}{H_{max}}$$

where $H_{max} = H(U) = \log(N_b)$ is the maximum possible entropy, achieved for a uniform distribution U ($p_j = 1/N_b$ for all j). Thus, $MI = 0$ when the phase-amplitude distribution is uniform, and $MI = 1$ in the (hypothetical) case in which gamma only appears in one phase bin of theta ($p_k = 1$ for a single bin k, and $p_j = 0$ for all $j \neq k$).

The MI is related to the Kullback-Leibler divergence (D_{KL}) by the equation $D_{KL}(P, U) = \log(N_b) - H(P)$. In other words, the MI can be viewed as the normalized Kullback-Leibler divergence between the uniform distribution and the observed phase-amplitude distribution:

$$MI = \frac{D_{KL}(P,U)}{H_{max}}$$

In practical terms, a Dirac-like distribution is improbable for real LFP signals and the MI values are skewed towards zero. In LFP recordings, significant theta-gamma MI values usually lie

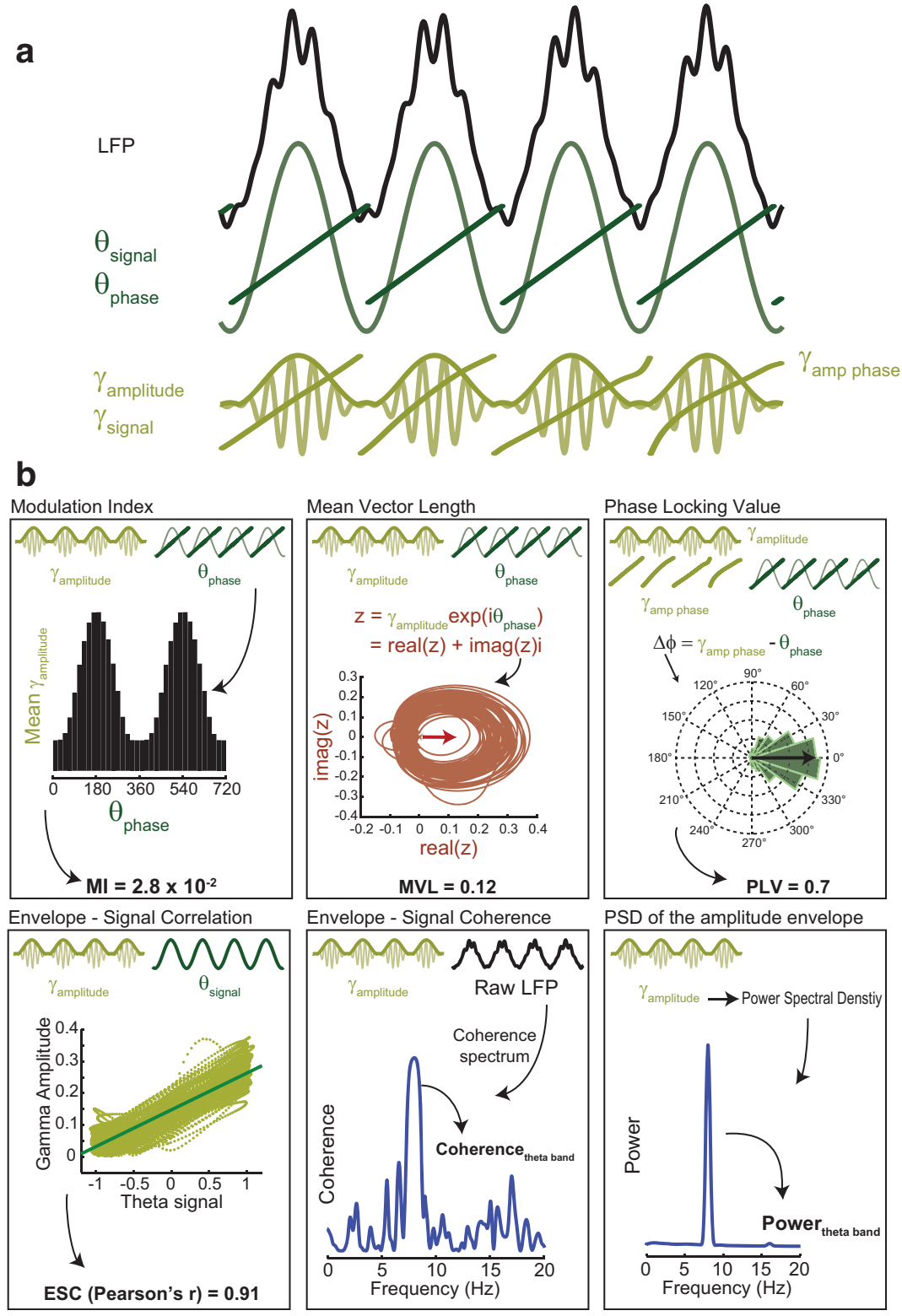

Fig. 2 (continued)

between 10^{-3} and 10^{-2}; values around 10^{-4} are considered weak and may be borderline for statistical significance, especially for short epochs. The MI can also be computed using the distribution of gamma bursts, that is, the counts of events per theta phase where gamma amplitude is higher than a threshold.

Mean Vector Length (MVL)

Canolty et al. (2006) introduced a PAC metric based on the complex time series $A_\gamma(t)e^{i\varphi_\theta(t)}$, where $A_\gamma(t)$ is the instantaneous gamma amplitude at time t and $\varphi_\theta(t)$ the instantaneous theta phase. The existence of PAC can be visually inferred by plotting these vectors in the complex plane: if theta and gamma are phase-amplitude coupled, the higher gamma amplitude in a subset of theta phases leads to an asymmetric distribution of vector lengths (amplitude values) around the origin. PAC strength can be estimated by measuring this asymmetry by means of the length of the mean vector:

$$PAC_{strength} = \left| \frac{1}{N} \sum_{j=1}^{N} A_\gamma(t_j) e^{i\varphi_\theta(t_j)} \right|$$

where N is the number of time points. The absence of PAC is characterized by a roughly uniform circular distribution of individual vectors, which will cancel each other out and lead to a low MVL. On the other hand, an asymmetry (polarization) in the complex plane leads to a resultant mean vector of larger length. The larger the polarization, the larger the MVL.

In the original formulation, the MVL was normalized and expressed as z-score in relation to a surrogate distribution of 200 MVL values (obtained from $A_\gamma(t)$ and $\varphi_\theta(t)$ not matched in time) (Canolty et al. 2006). Thus, the normalized metric reflected the statistical significance of PAC more than its strength.

Phase-locking Value (PLV)

In addition to being used to assess phase synchrony (Lachaux et al. 1999), the PLV can be readily adapted to measure PAC strength (Vanhatalo et al. 2004; Cohen 2008; Penny et al. 2008). As the MVL, the PLV also relies on computing the length of a mean vector, but in this case the time series is composed of unitary vectors. To compute the PLV, the instantaneous gamma amplitude must be first demeaned (or detrended), so that it assumes positive and negative values. For the case of a theta-modulated gamma, the demeaned amplitude time-series oscillates around zero at theta frequency. The PLV is the length of the mean over unit vectors whose angle is the difference between the phase of theta (φ_θ) and the phase of gamma amplitude (φ_{A_γ}):

$$PAC_{strength} = \left| \frac{1}{N} \sum_{j=1}^{N} e^{i\Delta\varphi(t_j)} \right|$$

where $\Delta\varphi(t_j) = \varphi_{A_\gamma}(t_j) - \varphi_\theta(t_j)$. The more the gamma amplitude is phase-locked to theta, the more constant their phase difference is. The PLV is 1 if $\Delta\varphi(t_j)$ is exactly constant for all t, and 0 if the circular distribution of phase differences is uniform.

Envelope-Signal Correlation (ESC)

The ESC metric is the correlation between the theta-filtered signal (x_θ) and the amplitude envelope of gamma (A_γ) (Bruns and Eckhorn 2004):

$$PAC_{strength} = \mathrm{corr}(x_\theta, A_\gamma) = \frac{1}{N} \sum_{j=1}^{N} \frac{(x_\theta(t_j) - \overline{x_\theta})(A_\gamma(t_j) - \overline{A_\gamma})}{\sigma_{x_\theta}\sigma_{A_\gamma}}$$

Penny et al. (2008) introduced a variation that normalizes for the amplitude of theta, which is achieved by correlating gamma amplitude with

Theta-Gamma Cross-Frequency Analyses (Hippocampus), Fig. 2 Diversity of PAC metrics. (**a**) Simulated signal containing theta and gamma oscillations in which theta phase modulates gamma amplitude. The phase of the gamma amplitude time series is extracted after demeaning. (**b**) Panels depict different measures for PAC (see text)

the cosine of the instantaneous theta phase ($\cos(\varphi_\theta)$):

$$PAC_{strength} = \mathrm{corr}\left(\cos\left(\varphi_\theta\right), A_\gamma\right)$$

The correlation metrics vary between −1 and 1; when gamma amplitude is maximal near the trough of theta, the correlation is negative, while positive correlations occur when gamma amplitude is maximal near the theta peak. The correlation may be zero even in the presence of phase-amplitude coupling if gamma has maximal amplitude when theta crosses zero (i.e., at 90° from the cycle peak or trough), the so-called "null phases" (Cohen 2008; Penny et al. 2008; Tort et al. 2010).

General Linear Model (GLM)

To circumvent the fact that the correlation metrics are not well suited to detect coupling if gamma is maximal at the null phases (i.e., zero crossings at $\cos(\pi/2)$ and $\cos(3\pi/2)$), Penny et al. (2008) proposed a generalization using GLM. In this framework, gamma amplitude is modeled as:

$$A_\gamma = \beta_0 + \beta_1 cos\left(\varphi_\theta\right) + \beta_2 sin\left(\varphi_\theta\right) + \varepsilon$$

where β_j ($j = 0,1,2$) are the regression coefficients and ε is the error (noise) term. Since the sine and cosine of the same phase is never simultaneously zero, the GLM metric has no "null phases." Finding the regression coefficients can be achieved by standard linear regression techniques. The GLM-based PAC metric is then defined as:

$$PAC_{strength} = \frac{SS\left(A_\gamma\right) + SS(\varepsilon)}{SS\left(A_\gamma\right)}$$

where $SS(A_\gamma)$ is the explained sum of squares of the model and $SS(\varepsilon)$ the sum of squared errors (residuals).

Envelope-Signal Coherence

PAC can also be estimated from the coherence spectra between the instantaneous gamma amplitude time series and the unfiltered LFP signal (Colgin et al. 2009). The standard (i.e., Fourier-based) phase coherence between two signals X and Y is defined as:

$$C_{XY}(f) = \frac{\left\| < F_X(f) \cdot \overline{F_Y(f)} > \right\|}{\| < F_X(f) > \| \| < F_Y(f) > \|}$$

where $F_X(f)$ and $F_Y(f)$ are the Fourier transforms at frequency f of X and Y, respectively. Oftentimes the "magnitude-squared" coherence ($C_{XY}{}^2$) is used. Both C_{XY} and $C_{XY}{}^2$ vary between 0 and 1. A theta-gamma coupling metric can then be obtained as the average coherence in the theta frequency range.

Power Spectral Density (PSD) of the Amplitude Envelope

If phase-modulated by theta, gamma amplitude tends to oscillate at theta frequency. Therefore, decomposing A_γ into its frequency components by means of Fourier spectral analysis may be used to infer PAC (Cohen 2008; Tort et al. 2010). Similarly to the coherence metric above, in this framework PAC is estimated by integrating (or averaging) the PSD of A_γ over the theta range. Such a method may provide meaningless estimates if the A_γ PSD has no peak at theta frequency.

Mutual Information

Theta-gamma PAC can be assessed using Shannon's mutual information, which computes how much the joint probability of phase and amplitude values deviates from the product of their marginal distributions. By definition, mutual information is zero for independent variables (joint probability equal to the product of the marginal probabilities). To estimate the joint and marginal probability distributions, the range of phase (i.e., 0 to 2π) and amplitude values must be first binned; each bin count is subsequently normalized by the total counts (N_{total} = sampling rate × epoch length), yielding:

$$p(\varphi_i) = \frac{N_{\varphi_i}}{N_{\text{total}}}, p\left(a_j\right) = \frac{N_{a_j}}{N_{\text{total}}}, \text{ and}$$

$$p(\varphi_i, a_j) = \frac{N_{\varphi_i \cap a_j}}{N_{\text{total}}},$$

where N_{φ_i} is the number of counts in phase bin i, N_{a_j} the number of counts in amplitude bin j, and $N_{\varphi_i \cap a_j}$ the number of joint counts. Mutual information is then estimated as:

$$PAC_{strength} = I(\Phi;A) = \sum_{i=1}^{M_b}\sum_{j=1}^{N_b} p(\varphi_i, a_j)\log\left(\frac{p(\varphi_i, a_j)}{p(\varphi_i)p(a_j)}\right)$$

where M_b and N_b are the number of phase and amplitude bins, respectively. This estimator is considered naïve since it does not correct for the positive bias associated with the use of finite samples to estimate the probability distributions; more sophisticated estimators that correct for such bias can be used (Panzeri et al. 2007).

Comodulation Maps

Comodulation maps, or "comodulograms," are 2D heatmaps that simultaneously express PAC strength values for multiple frequency pairs, and can be constructed for any of the metrics above (Fig. 3). Usually, the x-axis represents the phase-providing frequency and the y-axis the amplitude-modulated frequency, while the color represents PAC strength. In some cases, the color represents the statistical significance of PAC.

Phase-Phase Coupling (PPC)

Cross-frequency PPC is defined as a consistent phase relation between multiple gamma cycles within theta cycles. This type of CFC is also called n:m phase-locking. For example, 1:5 phase-locking is characterized by five gamma cycles consistently nested within theta cycles, in which each gamma cycle (i.e., the first, the second, etc.) starts/finishes at a similar theta phase across cycles. In PPC, theta and gamma would adjust their instantaneous frequencies in order to keep the same ratio of cycles; therefore, PPC can also be considered as frequency locking.

Mean Radial Distance ($R_{n:m}$)

The mean radial distance ($R_{n:m}$) – also called mean resultant length – is a common metric of PPC strength. This metric is similar to the PLV, but with phasors defined as unitary vectors whose angle is the phase difference between accelerated theta and gamma phases (Tass et al. 1998):

$$PPC_{strength} = R_{n:m} = \left|\left|\frac{1}{N}\sum_{j=1}^{N} e^{i\Delta\varphi_{nm}(t_j)}\right|\right|$$

where $\Delta\varphi_{nm}(t_j) = n\varphi_\gamma(t_j) - m\varphi_\theta(t_j)$, and $n\varphi_\gamma$ ($m\varphi_\theta$) represents the phase of gamma (theta) accelerated n (m) times. In the case of theta-gamma PPC, $R_{n:m}$ "curves" are usually obtained by varying m with $n = 1$ (Belluscio et al. 2012; Scheffer-Teixeira and Tort 2016). PPC strength can also be expressed for multiple n and m values by means of 2D heatmaps (Palva et al. 2005).

Shannon Entropy–Based Index

Tass et al. (1998) proposed two metrics of n:m phase-locking. One of the metrics is defined as an inverted normalization of the Shannon entropy of the probability distribution of $\Delta\varphi_{nm}$ (Ψ_{nm}):

$$PPC_{strength} = \frac{H_{max} - H(\Psi_{nm})}{H_{max}}$$

where H_{max} is the entropy of the circular uniform distribution. The probability distribution Ψ_{nm} is estimated by binning the circle into non-overlapping phase bins, counting the number of $\Delta\varphi_{nm}$ values within each bin, and normalizing the bin counts by the total counts. Notice that this metric is essentially the same as the PAC MI (actually, the latter was adapted from the former), but applied to the circular distribution of phase difference values instead of amplitude values.

Conditional Probability-Based Index

The second measure introduced by Tass et al. (1998) relies on assessing instantaneous gamma phases conditioned to fixed theta phase bins. In this framework, the theta phases are first binned

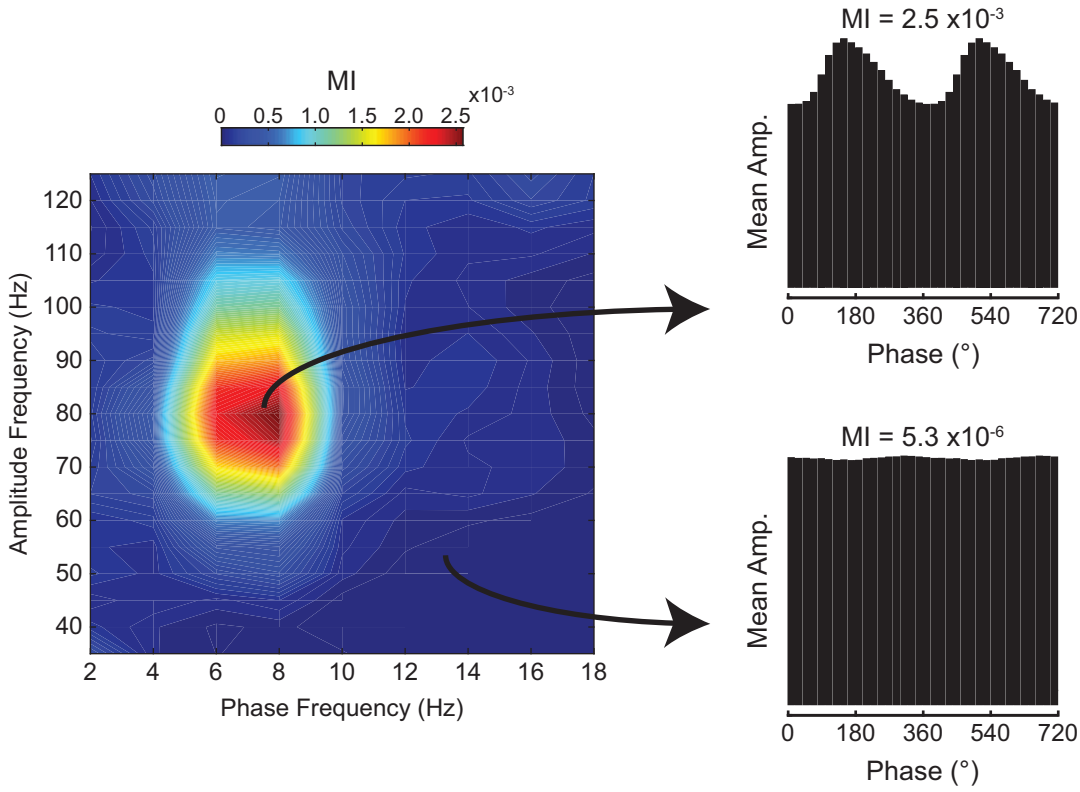

Theta-Gamma Cross-Frequency Analyses (Hippocampus), Fig. 3 Comodulation maps. PAC strength for several pairs of phase- and amplitude-providing frequency ranges can be simultaneously depicted by means of a bidimensional pseudocolor map, in which the color scale denotes the value of the PAC metric (in this example, the MI). The coordinates usually represent the center frequency of the filtered signals. Comodulation maps can also be constructed for other CFC types

into N_θ nonoverlapping bins; then, the following vector is computed for each phase bin θ_l:

$$R_{\theta_l} = \frac{\sum_{j=1}^{N_l} e^{i\varphi_\gamma(t_j)}}{N_l}$$

where $\varphi_\gamma(t_j)$ is the instantaneous gamma phase at t_j, and N_l is the total number of timestamps t_j belonging to θ_l (i.e., t_j is such that $\varphi_\theta(t_j) \in \theta_l$). Therefore, each theta phase bin is associated with a mean vector over phasors whose angles are the instantaneous gamma phases falling in it. If gamma has the exact same phase within a fixed theta phase bin, the magnitude of R_{θ_l} is 1. On the other hand, if $\varphi_\gamma(t_j)$ values are random (i.e., gamma is not phase-locked), the unit vectors will cancel each other out, and $|R_{\theta_l}|$ will be small. The PPC metric is defined as the average vector length over all theta phase bins:

$$PPC_{strength} = \frac{\sum_{l=1}^{N_\theta} |R_{\theta_l}|}{N_\theta}$$

Pairwise Phase-Consistency

Phase-locking metrics based on the addition of phase difference vectors are positively biased for small samples. To circumvent this issue, Vinck et al. (2010) proposed the pairwise phase consistency, which is defined as the average dot product over all vector pairs, or, equivalently, the average cosine between all vector pairs. Scheffer-Teixeira and Tort (2016) recently used Vinck's metric to measure n:m phase-locking by applying it to the

difference between accelerated gamma and theta phases ($\Delta\varphi_{nm}$):

$$PPC_{strength} = \frac{2}{N(N-1)} \sum_{j=1}^{N-1} \sum_{k=(j+1)}^{N} \cos\left(\Delta\varphi_{nm}(t_j) - \Delta\varphi_{nm}(t_k)\right)$$

where N is the total number of time samples. If the accelerated phase differences $\Delta\varphi_{nm}$ are constant, meaning perfect n:m phase-locking, $\cos(\Delta\varphi_{nm}(t_j) - \Delta\varphi_{nm}(t_k)) = \cos(0) = 1$ and consequently PPC = 1. If $\Delta\varphi_{nm}$ values are random and uniformly distributed over the circle, the expected value of PPC is 0.

Mutual Information

Theta-gamma PPC can also be measured using Shannon's mutual information in a similar way as described above for PAC assessment. Namely, the joint and marginal probability distributions are first estimated from phase bin counts (N_{total} = sampling rate × epoch length):

$$p\left(\varphi_{\theta_i}\right) = \frac{N_{\theta_i}}{N_{\text{total}}}, p\left(\varphi_{\gamma_j}\right) = \frac{N_{\varphi_{\gamma_j}}}{N_{\text{total}}}, \text{ and}$$

$$p\left(\varphi_{\theta_i}, \varphi_{\gamma_j}\right) = \frac{N_{\varphi_{\theta_i} \cap \varphi_{\gamma_j}}}{N_{\text{total}}},$$

and mutual information is subsequently calculated as:

$$PPC_{strength} = I\left(\Phi_\theta; \Phi_\gamma\right)$$

$$= \sum_{i=1}^{M} \sum_{j=1}^{N} p\left(\varphi_{\theta_i}, \varphi_{\gamma_j}\right) \log\left(\frac{p\left(\varphi_{\theta_i}, \varphi_{\gamma_j}\right)}{p\left(\varphi_{\theta_i}\right) p\left(\varphi_{\gamma_j}\right)}\right)$$

Amplitude–Amplitude Coupling (AAC)

Correlation Between Amplitude or Power Values

Theta-gamma AAC can be estimated as the correlation between the amplitude envelopes of theta (A_θ) and gamma (A_γ) (Bruns et al. 2000; Bruns and Eckhorn 2004):

$$AAC_{strength} = \text{corr}\left(A_\theta, A_\gamma\right) = \frac{1}{N} \sum_{j=1}^{N} \frac{\left(A_\theta(t_j) - \overline{A_\theta}\right)\left(A_\gamma(t_j) - \overline{A_\gamma}\right)}{\sigma_{A_\theta} \sigma_{A_\gamma}}$$

Alternatively, the correlation can be performed using integrated power over the desired frequency ranges. To that end, the analyzed epoch must be first partitioned into contiguous, nonoverlapping windows and Fourier-transformed within windows to compute the power spectra (Masimore et al. 2004). With either framework, an amplitude-amplitude comodulogram can be plotted by representing the correlation coefficients of multiple frequency pairs by means of a 2D heatmap (Masimore et al. 2004).

Phase-Locking of Amplitude Envelopes

The phase-locking value (PLV) can also be adapted to measure AAC (Jirsa and Müller 2013). Instead of using the filtered signal, the phase time series are extracted from the detrended amplitude envelopes of theta (A_θ) and gamma (A_γ). AAC is then estimated as:

$$AAC_{strength} = \left\| \frac{1}{N} \sum_{j=1}^{N} e^{i\left(\varphi_{A_\theta}(t_j) - \varphi_{A_\gamma}(t_j)\right)} \right\|$$

Mutual Information

As all CFC types, theta-gamma AAC can also be assessed by mutual information. To that end, the range of amplitude values of each oscillation must be binned into nonoverlapping bins. Estimations of the joint and marginal probability of amplitude values are then obtained by normalizing bin counts and used to compute the mutual information.

Phase–Frequency Coupling (PFC), Amplitude-Frequency Coupling (AFC), and Frequency-Frequency Coupling (FFC)

PFC, AFC, and FFC have been considerably less explored than the other CFC types (Hyafil et al. 2015). Nevertheless, several of the metrics described above can be adapted to measure these interactions. For instance, Hyafil (2015) proposed that standard PAC measures could assess PFC by

using the instantaneous frequency time series instead of the amplitude envelope. More generally, the values achieved by each oscillatory feature (e.g., amplitude or frequency) can always be binned and transformed into probability distributions to allow for computing the mutual information.

Sources of Biases and Spurious Coupling

There are several possible sources of bias and spurious results in CFC research (Kramer et al. 2008; Aru et al. 2015; Hyafil 2015; Scheffer-Teixeira and Tort 2016); among them:

1. *Asymmetric waveform*: recent studies have explored the influence of waveform shape on CFC measures (Gerber et al. 2016; Lozano-Soldevilla et al. 2016; Scheffer-Teixeira and Tort 2016; Cole et al. 2017). For instance, hippocampal theta oscillations are asymmetric, in that the rising phase is faster than the falling one, and such asymmetry increases with locomotion speed (Belluscio et al. 2012). Waveform asymmetry may induce spurious PAC and PPC, since the filtered signals will reflect a set of harmonic waves that naturally couple to the fundamental oscillation and to each other (Aru et al. 2015; Scheffer-Teixeira and Tort 2016). Another side-effect of asymmetric waveforms is nonuniform phase distributions, which may produce biased CFC estimates (van Driel et al. 2015).
2. *Sharp edges*: Kramer et al. (2008) recognized that sharp signal deflections are a potential confound factor in CFC analyses. The sharp edges in EEG and LFP signals may have either biological origin (e.g., event-related potentials or spike-and-wave mu rhythms) or be due to stimulation artifacts. At any event, the abrupt deflections give rise to spurious fast oscillatory activity in filtered signals, which in turn may mislead CFC estimates.
3. *Nonmeaningful features and filtering-induced sinusoidality*: standard filtering methods tend to produce sinusoid-like signals even in the absence of genuine brain oscillations in the filtered frequency range. As a consequence of the sinusoidality imposed by the filter, the phase and frequency time series may temporally appear as coupled and lead to PPC overestimation, especially in short time epochs (Scheffer-Teixeira and Tort 2016; Hyafil 2017).
4. *Wrong bandwidth choice*: In PAC analysis, the filtered bandwidth should contain both the amplitude-modulated frequency and the side bands (modulated frequency $\pm$ modulating frequency). Therefore, narrowly filtered frequency bands may not detect genuine PAC (Berman et al. 2012; Aru et al. 2015). Curiously, however, Hyafil (2015) pointed out that PFC can be mistaken as PAC in narrowly filtered signals, since cyclic variations of the instantaneous gamma frequency outside the filtered range will be associated with cyclic amplitude variations. For a similar reason, Hyafil (2015) further pointed out that variations in instantaneous frequency may be mistaken as AAC.
5. *Phase slips and frequency spikes*: Instantaneous frequency is estimated as the first derivative of the phase time series. Fast signal perturbations may cause "jumps" in the phase time series, the so-called "phase slips" (Hurtado et al. 2004). Such events produce large deviations of the instantaneous frequency ("frequency spikes"), much above or below the filtered frequency range (it may even assume negative values), even though the frequency of the rhythm may not change on a larger timescale (see Fig. 1A for an actual example). Of note, phase slips and frequency spikes are also common in aperiodic or noisy signals. Abundant phase slips may thus bias the assessment of frequency coupling. One method to overcome this issue is to detect the associated frequency spikes and smooth them out (Hurtado et al. 2004).

Ideally, the investigated oscillations (i.e., theta and gamma) should exist in the analyzed signal, as inferred by peaks in the power frequency spectrum. As a rule of thumb, CFC estimates are most "trustable" when one can observe such interaction by visual inspection of raw (unfiltered) signals. Theta- and gamma-filtered signals can be plotted along with the unfiltered signal to facilitate such inspection.

Statistical Assessment

Statistical analyses may be used to infer if CFC exists (i.e., beyond chance levels) or to compare CFC strength among different groups (e.g., different manipulations, cognitive states, frequency pairs, or brain regions). While the latter can be performed with standard statistical tests, the former usually requires the construction of surrogate distributions of coupling strength. As a general rule, a good surrogate method should preserve data continuity and spectral properties, as well as it should use the same epoch length as the original data (Scheffer-Teixeira and Tort 2016). A typical surrogate procedure is to analyze theta and gamma time series not matched in time. The existence of theta-gamma coupling is then assessed by comparing the actual CFC metric with the chance distribution of surrogate values.

On the Choice of the CFC Metric

As summarized above, several CFC metrics were proposed to quantify the presence or absence of interacting brain oscillations. However, the repertoire of metrics may lead to confusion when choosing one of them, which motivated some comparative studies (e.g., Penny et al. 2008; Tort et al. 2010; Onslow et al. 2011). As a starting point, one can assume that a good metric should present (1) unbiased estimators, (2) tolerance to noise, and (3) strength representation (i.e., different coupling levels are separately represented by the metric). Regarding these characteristics, we make the following observations:

(1) Vinck et al. (2010) showed that the metrics based on vector addition, such as MVL, PLV, and coherence, are positively biased for shorter epochs. (Although Vinck et al. have originally referred to phase synchrony metrics devised for oscillations of the same frequency, these metrics were eventually adapted to measure PAC and inherited the same caveats.) This is because – in the absence of coupling – a large enough number of vectors should be sampled to produce a null resultant vector. But we note that the positive bias for short epochs is not unique to these metrics. In general, to confidently assess PAC, one needs to analyze enough cycles to infer whether consistent variations of the gamma amplitude exist within theta cycles. In practice, the instantaneous gamma amplitude is never constant within the time window of a theta cycle (~125 ms), and hence, a phase-amplitude distribution computed using a single theta cycle will never be uniform. Therefore, the presence of nonuniform phase-amplitude distributions should be interpreted with caution for short time epochs and, most importantly, must be compared with chance distributions (c.f., last section above). While we cannot advocate a minimal epoch length for CFC analysis due to the great variability of brain signals, metrics, and research settings, we recommend always to perform internal checks using real and simulated data, such as to assess metric convergence as a function of the analyzed epoch length and chance distributions (Tort et al. 2010; Scheffer-Teixeira and Tort 2016).

(2) The addition of noise to phase-amplitude coupled signals may differentially affect some PAC metrics. Tort et al. (2010) found that PLV, ESC, GLM, and coherence are negatively affected by noise, which leads them to underestimate PAC strength. On the other hand, the ratio-based metrics, MI and MVL, are more tolerant to noise, while the amplitude PSD overestimates PAC strength with higher noise levels. This occurs because the added noise increases power in all frequency bands.

(3) Some measures may better track "coupling consistency" across cycles, defined as the proportion of theta cycles in which gamma appears modulated by theta, but are less sensitive to "coupling strength," defined as the magnitude of the amplitude modulation

within theta cycles (Tort et al. 2010). For instance, PLV and coherence both are based on the phase transformation of the gamma amplitude. Because of that, the amplitude modulations will be treated as cycles with phases varying from 0° to 360°, irrespective of the magnitude (e.g., an amplitude variation of ± 10% or ± 50% from the mean may lead to similar phase time series). Correlation-based indexes, such as GLM and ESC, also do not represent the coupling strength well, but for a different reason: the presence of higher modulations shifts the regression slope or the Y-intercept, but does not necessarily change the correlation/regression coefficient (Tort et al. 2010). Finally, by design, some PAC metrics such as the MVL and the amplitude PSD take into account the absolute amplitude of gamma and will thus also depend on gamma power irrespective of the "relative" coupling strength, as defined by the percentage of change from the mean amplitude (Tort et al. 2010).

Of note, some may also be interested that the metric is capable of detecting multimodal coupling (e.g., when gamma amplitude has two maxima within a theta cycle). By their definitions, the MI and the mutual information would be better suited in these cases (Tort et al. 2010).

Despite these particularities, it should be noted that hippocampal theta-gamma PAC is usually a phenomenon robust enough to be detected by any of the metrics. Ultimately, one should choose a metric whose advantages and limitations are well understood, and also bear in mind that the very definition of CFC will depend on this choice. In this sense, since it is presently unclear whether the assessment of "coupling consistency" or "coupling strength" (c.f. definitions above) would be cognitively more relevant, we cannot point to a single PAC metric as the best one.

Lastly, we note that PPC has received less attention regarding comparative studies among metrics. Shannon entropy, conditional probability, and mutual information-based indexes are not as widely used as the mean radial distance. The mean radial distance, however, is based on vector addition and is thus a positively biased estimator (small epochs result in higher values). Recently, Scheffer-Teixeira and Tort (2016) showed computationally that Vinck's pairwise phase consistency could be adapted and used as an unbiased index for PPC.

Novel CFC Metrics

The study of cross-frequency interactions is an active field of research, which involves scientists working at different levels, brain regions, species, and brain signals (e.g., EEG, ECOG, LFP, MEG). CFC has also been described outside the brain, such as in the gut (Huizinga et al. 2014), and also in non-biological fields such as atmospheric dynamics (Paluš 2014). As an active field, new CFC metrics are continuously being elaborated; there are certainly far more CFC metrics than the ones summarized in this chapter. Important advances include metrics designed to infer coupling directionality (Paluš 2014; Jiang et al. 2015; Li et al. 2016), to improve time-resolution (Voytek et al. 2013; Dvorak and Fenton 2014; Samiee and Baillet 2017), to provide confidence intervals and higher statistical rigor (Kramer and Eden 2013; van Wijk et al. 2015), to avoid standard filters by using autoregressive models (Tour et al. 2017) or empirical mode decomposition (Pittman-Polletta et al. 2014), and to cope with multiple channel data and spatial filtering (Cohen 2017).

Cross-References

▶ Hippocampus, Theta, Gamma, and Cross-Frequency Coupling

References

Aru J, Aru J, Priesemann V, Wibral M, Lana L, Pipa G, Singer W, Vicente R (2015) Untangling cross-frequency coupling in neuroscience. Curr Opin Neurobiol 31:51–61

Belluscio MA, Mizuseki K, Schmidt R, Kempter R, Buzsáki G (2012) Cross-frequency phase-phase coupling between θ and γ oscillations in the hippocampus.

J Neurosci 32:423–435. https://doi.org/10.1523/JNEUROSCI.4122-11.2012
Berman JI, McDaniel J, Liu S, Cornew L, Gaetz W, Roberts TPL, Edgar JC (2012) Variable bandwidth filtering for improved sensitivity of cross-frequency coupling metrics. Brain Connect 2:155–163. https://doi.org/10.1089/brain.2012.0085
Bruns A, Eckhorn R (2004) Task-related coupling from high- to low-frequency signals among visual cortical areas in human subdural recordings. Int J Psychophysiol 51:97–116
Bruns A, Eckhorn R, Jokeit H, Ebner A (2000) Amplitude envelope correlation detects coupling among incoherent brain signals. Neuroreport 11:1509–1514
Buzsáki G (2002) Theta oscillations in the hippocampus. Neuron 33:325–340
Canolty RT, Knight RT (2010) The functional role of cross-frequency coupling. Trends Cogn Sci 14:506–515. https://doi.org/10.1016/j.tics.2010.09.001
Canolty RT, Edwards E, Dalal SS, Soltani M, Nagarajan SS, Kirsch HE, Berger MS, Barbaro NM, Knight RT (2006) High gamma power is phase-locked to theta oscillations in human neocortex. Science 313:1626–1628. https://doi.org/10.1126/science.1128115
Cohen MX (2008) Assessing transient cross-frequency coupling in EEG data. J Neurosci Methods 168:494–499. https://doi.org/10.1016/j.jneumeth.2007.10.012
Cohen MX (2017) Multivariate cross-frequency coupling via generalized eigendecomposition. eLife 6:e21792. https://doi.org/10.7554/eLife.21792
Cole SR, van der Meij R, Peterson EJ, de Hemptinne C, Starr PA, Voytek B (2017) Nonsinusoidal beta oscillations reflect cortical pathophysiology in Parkinson's disease. J Neurosci 37:4830–4840. https://doi.org/10.1523/JNEUROSCI.2208-16.2017
Colgin LL, Denninger T, Fyhn M, Hafting T, Bonnevie T, Jensen O, Moser M-B, Moser EI (2009) Frequency of gamma oscillations routes flow of information in the hippocampus. Nature 462:353–357
Dvorak D, Fenton AA (2014) Toward a proper estimation of phase-amplitude coupling in neural oscillations. J Neurosci Methods 225:42–56. https://doi.org/10.1016/j.jneumeth.2014.01.002
Ermentrout GB, Kopell N (1991) Multiple pulse interactions and averaging in systems of coupled neural oscillators. J Math Biol 29:195–217. https://doi.org/10.1007/BF00160535
Geddes LA (1987) What did Caton see? Electroencephalogr Clin Neurophysiol 67:2–6
Gerber EM, Sadeh B, Ward A, Knight RT, Deouell LY (2016) Non-sinusoidal activity can produce cross-frequency coupling in cortical signals in the absence of functional interaction between neural sources. PLoS One 11:e0167351. https://doi.org/10.1371/journal.pone.0167351
Hoppensteadt FC, Izhikevich EM (1998) Thalamo-cortical interactions modeled by weakly connected oscillators: could the brain use FM radio principles? Biosystems 48:85–94
Huizinga JD, Chen J-H, Zhu YF, Pawelka A, McGinn RJ, Bardakjian BL, Parsons SP, Kunze WA, Wu RY, Bercik P, Khoshdel A, Chen S, Yin S, Zhang Q, Yu Y, Gao Q, Li K, Hu X, Zarate N, Collins P, Pistilli M, Ma J, Zhang R, Chen D (2014) The origin of segmentation motor activity in the intestine. Nat Commun 5:3326. https://doi.org/10.1038/ncomms4326
Hurtado JM, Rubchinsky LL, Sigvardt KA (2004) Statistical method for detection of phase-locking episodes in neural oscillations. J Neurophysiol 91:1883–1898. https://doi.org/10.1152/jn.00853.2003
Hyafil A (2015) Misidentifications of specific forms of cross-frequency coupling: three warnings. Front Neurosci 9:370. https://doi.org/10.3389/fnins.2015.00370
Hyafil A (2017) Disharmony in neural oscillations. J Neurophysiol 118:1–3. https://doi.org/10.1152/jn.00026.2017
Hyafil A, Giraud A-L, Fontolan L, Gutkin B (2015) Neural cross-frequency coupling: connecting architectures, mechanisms, and functions. Trends Neurosci 38:725–740. https://doi.org/10.1016/j.tins.2015.09.001
Jiang H, Bahramisharif A, van Gerven MAJ, Jensen O (2015) Measuring directionality between neuronal oscillations of different frequencies. NeuroImage 118:359–367. https://doi.org/10.1016/j.neuroimage.2015.05.044
Jirsa V, Müller V (2013) Cross-frequency coupling in real and virtual brain networks. Front Comput Neurosci 7. https://doi.org/10.3389/fncom.2013.00078
Kramer MA, Eden UT (2013) Assessment of cross-frequency coupling with confidence using generalized linear models. J Neurosci Methods 220:64–74. https://doi.org/10.1016/j.jneumeth.2013.08.006
Kramer MA, Tort ABL, Kopell NJ (2008) Sharp edge artifacts and spurious coupling in EEG frequency comodulation measures. J Neurosci Methods 170:352–357. https://doi.org/10.1016/j.jneumeth.2008.01.020
la Tour TD, Tallot L, Grabot L, Doyère V, van Wassenhove V, Grenier Y, Gramfort A (2017) Non-linear auto-regressive models for cross-frequency coupling in neural time series. PLoS Comput Biol 13:e1005893. https://doi.org/10.1371/journal.pcbi.1005893
Lachaux J-P, Rodriguez E, Martinerie J, Varela FJ (1999) Measuring phase synchrony in brain signals. Hum Brain Mapp 8:194–208
Lakatos P, Shah AS, Knuth KH, Ulbert I, Karmos G, Schroeder CE (2005) An oscillatory hierarchy controlling neuronal excitability and stimulus processing in the auditory cortex. J Neurophysiol 94:1904–1911. https://doi.org/10.1152/jn.00263.2005
Li Q, Zheng C-G, Cheng N, Wang Y-Y, Yin T, Zhang T (2016) Two generalized algorithms measuring phase-amplitude cross-frequency coupling in neuronal oscillations network. Cogn Neurodyn 10:235–243. https://doi.org/10.1007/s11571-015-9369-6

Lozano-Soldevilla D, Ter Huurne N, Oostenveld R (2016) Neuronal oscillations with non-sinusoidal morphology produce spurious phase-to-amplitude coupling and directionality. Front Comput Neurosci 10:87. https://doi.org/10.3389/fncom.2016.00087

Masimore B, Kakalios J, Redish AD (2004) Measuring fundamental frequencies in local field potentials. J Neurosci Methods 138:97–105. https://doi.org/10.1016/j.jneumeth.2004.03.014

Onslow ACE, Bogacz R, Jones MW (2011) Quantifying phase–amplitude coupling in neuronal network oscillations. Prog Biophys Mol Biol 105:49–57. https://doi.org/10.1016/j.pbiomolbio.2010.09.007

Paluš M (2014) Multiscale atmospheric dynamics: cross-frequency phase-amplitude coupling in the air temperature. Phys Rev Lett 112:078702. https://doi.org/10.1103/PhysRevLett.112.078702

Palva JM, Palva S, Kaila K (2005) Phase synchrony among neuronal oscillations in the human cortex. J Neurosci 25:3962–3972. https://doi.org/10.1523/JNEUROSCI.4250-04.2005

Panzeri S, Senatore R, Montemurro MA, Petersen RS (2007) Correcting for the sampling bias problem in spike train information measures. J Neurophysiol 98:1064–1072. https://doi.org/10.1152/jn.00559.2007

Penny WD, Duzel E, Miller KJ, Ojemann JG (2008) Testing for nested oscillation. J Neurosci Methods 174:50–61. https://doi.org/10.1016/j.jneumeth.2008.06.035

Pittman-Polletta B, Hsieh W-H, Kaur S, Lo M-T, Hu K (2014) Detecting phase-amplitude coupling with high frequency resolution using adaptive decompositions. J Neurosci Methods 226:15–32. https://doi.org/10.1016/j.jneumeth.2014.01.006

Rosenblum M, Pikovsky A, Kurths J, Schäfer C, Tass PA (2001) Chapter 9 phase synchronization: from theory to data analysis. In: Moss F, Gielen S (eds) Handbook of biological physics. North-Holland, Amsterdam, pp 279–321

Samiee S, Baillet S (2017) Time-resolved phase-amplitude coupling in neural oscillations. NeuroImage 159:270–279. https://doi.org/10.1016/j.neuroimage.2017.07.051

Scheffer-Teixeira R, Tort AB (2016) On cross-frequency phase-phase coupling between theta and gamma oscillations in the hippocampus. Elife 5:e20515. https://doi.org/10.7554/eLife.20515

Scheffer-Teixeira R, Tort ABL (2017) Unveiling fast field oscillations through comodulation eNeuro 4:ENEURO 0079-17.2017

Strogatz SH (2000) From Kuramoto to Crawford: exploring the onset of synchronization in populations of coupled oscillators. Phys Nonlinear Phenom 143:1–20. https://doi.org/10.1016/S0167-2789(00)00094-4

Tass P, Rosenblum MG, Weule J, Kurths J, Pikovsky A, Volkmann J, Schnitzler A, Freund H-J (1998) Detection of n: m phase locking from noisy data: application to magnetoencephalography. Phys Rev Lett 81:3291–3294

Tort ABL, Kramer MA, Thorn C, Gibson DJ, Kubota Y, Graybiel AM, Kopell NJ (2008) Dynamic cross-frequency couplings of local field potential oscillations in rat striatum and hippocampus during performance of a T-maze task. Proc Natl Acad Sci U S A 105:20517–20522. https://doi.org/10.1073/pnas.0810524105

Tort ABL, Komorowski R, Eichenbaum H, Kopell N (2010) Measuring phase-amplitude coupling between neuronal oscillations of different frequencies. J Neurophysiol 104:1195–1210. https://doi.org/10.1152/jn.00106.2010

van Driel J, Cox R, Cohen MX (2015) Phase-clustering bias in phase-amplitude cross-frequency coupling and its removal. J Neurosci Methods 254:60–72. https://doi.org/10.1016/j.jneumeth.2015.07.014

van Wijk BCM, Jha A, Penny W, Litvak V (2015) Parametric estimation of cross-frequency coupling. J Neurosci Methods 243:94–102. https://doi.org/10.1016/j.jneumeth.2015.01.032

Vanhatalo S, Palva JM, Holmes MD, Miller JW, Voipio J, Kaila K (2004) Infraslow oscillations modulate excitability and interictal epileptic activity in the human cortex during sleep. Proc Natl Acad Sci U S A 101:5053–5057. https://doi.org/10.1073/pnas.0305375101

Vinck M, van Wingerden M, Womelsdorf T, Fries P, Pennartz CMA (2010) The pairwise phase consistency: a bias-free measure of rhythmic neuronal synchronization. Neuro Image 51:112–122. https://doi.org/10.1016/j.neuroimage.2010.01.073

Voytek B, D'Esposito M, Crone N, Knight RT (2013) A method for event-related phase/amplitude coupling. NeuroImage 64:416–424. https://doi.org/10.1016/j.neuroimage.2012.09.023